

# Forecasting Significant Wave Heights in Oceanic Waters

Pujan Pokhrel

Canizaro Livingston Gulf States Center for  
Environmental Informatics  
New Orleans, LA 70148, USA.

Elias Ioup

Center for Geospatial Sciences,  
Naval Research Laboratory  
Stennis Space Center  
Mississippi, USA.

Md Tamjidul Hoque\*

Canizaro Livingston Gulf States Center for  
Environmental Informatics  
New Orleans, LA 70148, USA.

Mahdi Abdelguerfi

Canizaro Livingston Gulf States Center for  
Environmental Informatics  
New Orleans, LA 70148, USA.

Julian Simeonov

Ocean Sciences Division,  
Naval Research Laboratory  
Stennis Space Center  
Mississippi, USA.

\* To whom correspondence should be addressed: [thoque@uno.edu](mailto:thoque@uno.edu)

## ABSTRACT

This paper proposes a machine learning method based on the Extra Trees (ET) algorithm for forecasting Significant Wave Heights in oceanic waters. To derive multiple features from the CDIP buoys, which make point measurements, we first nowcast various parameters and then forecast them at 30-min intervals. The proposed algorithm has Scatter Index (SI), Bias, Correlation Coefficient, Root Mean Squared Error (RMSE) of 0.130, -0.002, 0.97, and 0.14, respectively, for one day ahead prediction and 0.110, -0.001, 0.98, and 0.122, respectively, for 14-day ahead prediction on the testing dataset. While other state-of-the-art methods can only forecast up to 120 hours ahead, we extend it further to 14 days. This 14-day limit is not the forecasting limit, but it arises due to our experiment's setup.

Our proposed setup includes spectral features, hv-block cross-validation, and stringent QC criteria. The proposed algorithm performs significantly better than the state-of-the-art methods commonly used for significant wave height forecasting for one-day ahead prediction. Moreover, the improved performance of the proposed machine learning method compared to the numerical methods, shows that this performance can be extended to even longer time periods allowing for early prediction of significant wave heights in oceanic waters.

## Keywords

Machine learning, ocean waves, significant wave height, prediction.

## 1. INTRODUCTION

This paper focuses on ocean waves' accurate prediction, which remains one of the most important outstanding classical physics problems [1]. The nowcasting and forecasting of waves are important for myriad reasons: optimizing ship routes for efficient shipping, avoiding disasters, aiding the aquaculture industry, safely conducting military and amphibious operations by Navy and Marine Corps teams, etc. The other importance of wave prediction lies in efficient renewable energy generated from renewable energy sources like solar, wind, tidal, wave, etc.

Commercialization and deployment of wave-energy technologies will require addressing regulatory matters and laws, as well as overcoming technological challenges like accurate and rapid forecasting of ocean conditions and incorporating relevant forecast data in its predictions.

Sverdrup and Munk [2] developed a statistical wave prediction technique based on the significant wave height. Later, numerical wave prediction methods using the coarse grid [3, 4], suitable for deepwater regions, were developed. However, the coarse grid methods do not yield better predictions on coastal areas, and thus, fine grid methods [4, 5] were developed. Examples of some third-generation numerical models include Simulating Waves Nearshore (SWAN) [6], and WAVEWATCH [5, 7-11], which have been widely applied in wave height forecasting.

Ocean waves are composed of various nonlinearities that lead to coupled Fourier modes, which need high-order spectral analysis or direct numerical simulations to examine, both of which are complex and time-consuming. Moreover, phase-resolved simulations may include the preprocessing step of calculating initial phases from the image representing sea surface elevation. Since the image snapshot contains the spectrum of different waves propagating in different directions, which can superimpose nonlinearly, calculating the images' wave parameters is time-consuming. They cannot be applied for real-time and fast prediction while carrying out maritime operations and feedback control application problems.

Further, numerical methods have low generalization ability, boundary conditions must be reset, and models run periodically for prediction in different regions. Despite considerable advances in computational techniques, numerical methods have not easily generalized over various sites and times due to complex parameters and high computational complexity [12].

To consider all the variables and reduce computational time, various machine learning methods have been proposed. Machine learning methods are data-driven and can statistically nowcast and forecast wave heights and other wave parameters. Data-driven methods can take more variables into account than the

numerical methods without an abrupt increase in computational complexity.

Various machine learning methods have been previously explored for the prediction of significant wave heights. Most of the methods used for nowcasting/forecasting significant wave heights can be divided into three groups: a) soft computing approaches (artificial neural networks, fuzzy inference systems, adaptive network-based fuzzy inference systems), b) kernel-based approaches like SVMs and, c) decision tree-based approaches.

Deo *et al.* [13] used Artificial Neural Networks (ANNs) to forecast wave height and period by using the generated wind speeds as inputs. Mahjoobi *et al.* [14, 15] used various soft computing approaches like artificial neural networks, fuzzy inference systems, and adaptive network-based fuzzy inference systems to hindcast various wave parameters. Their results show that all these approaches have similar performance. Furthermore, using sensitivity analysis, they showed that wind speed and direction are important parameters for nowcasting ocean wave heights. Afterward, Rizianiza *et al.* [16] developed an ANN-based model based on friction velocity, wind direction, significant wave height, wave direction, and improved forecast time to 24 hours. Moreover, a recent method by Elbisy *et al.* [17] uses ANN to predict daily tidal levels along the eastern Red Sea.

Similarly, Mahjoobi and Mosabbebi [14] used an SVM model to simulate the significant wave height for Lake Michigan by using current and previous wind speed data as inputs. Furthermore, Elbisy [18] combined SVM and genetic algorithms to predict significant wave height, wave direction, and peak spectral period in a coastal zone near the Nile Delta. Afterward, Duan [19] used WD-SVM to forecast significant wave height up to 6 hours and improved accuracy. The model used significant wave height as the input variable.

Likewise, Somayeh [20] used various variables like wind speed, significant wave height, wave period, pressure, air temperature, water temperature, and dew point to predict wave height for up to 24 hours based on the Random Forest method. Mahjoobi and Etemad-Shahidi [15] have used various data mining approaches to predict oceanic wave heights. They have proposed an alternative method for wave hindcasting based on classification and regression trees. The results of decision trees were compared with those of artificial neural networks. The errors of both models were similar, with a nearly equal amount of error. The authors argued that decision trees, with an acceptable range of error, could be used successfully for the prediction of significant wave heights and are better than neural networks in terms of interpretation since they represent rules.

Note that all the papers mentioned above use various features previously employed to nowcast and forecast significant wave heights. However, they did not use the stringent QC criteria to perform data filtering and get the highest quality training data. They also did not use the hv-blocked cross-validation scheme employed in this paper, which preserves the data's temporal ordering and helps get generalized performance for training machine learning methods in time series data. To address the shortcomings of the previous machine learning algorithms, we perform QC filtering and blocked cross-validation. This paper uses various machine learning algorithms to forecast wave heights in oceanic conditions. Specifically, we use Light Gradient Boosting (LightGBM) and Extra Trees (ET). LightGBM operates on boosting principle, and ET works on the bagging principle, which reduces bias error and variance error, respectively.

## 2. CALCULATION of VARIOUS WAVE PARAMETERS

### 2.1 Significant Wave Height ( $H_{m0}$ )

Significant Wave Height ( $H_{m0}$ ) is defined traditionally as the mean crest to trough height (mean wave height) of the highest third of the waves. It is also defined as four times the standard deviation of the surface elevation or four times the square root of the zeroth-order moment of the wave spectrum. All these definitions give similar results and may be used interchangeably.

$$H_{m0} = 4 * \sqrt{m_0} \quad (1)$$

$$m_0 = \sum_{i=0}^d E_i(f_i) * d(f_i) \quad (2)$$

where  $m_0$  is defined as the variance of the wave spectrum,  $E_i(f)$  is the spectral density at each frequency band,  $f_d$  is the dominant frequency at dominant frequency band  $d$ ,  $f_0$  refers to the lowest frequency measured by the buoys, which is 0.025 Hz, and  $d(f_i)$  is the bandwidth of each frequency band.

### 2.2 Dominant Wave Period ( $T_p$ )

The dominant wave period is defined as the period corresponding to the frequency band with the maximum value of spectral density in the nondirectional wave spectrum. It is calculated using the formula

$$D_p = \frac{1}{f_p} \quad (3)$$

where  $f_p$  is the peak frequency.

### 2.3 Mean Wave Period ( $T_a$ )

The mean crossing wave period is defined as the mean wave periods of the waves encountered during the wave sampling period. It is calculated using

$$D_p = \sqrt{\frac{m_0}{m_2}} \quad (4)$$

where  $m_2$  is defined as

$$m_2 = \sum_{i=0}^d (E_i(f_i) * d(f_i) * f_i^2) \quad (5)$$

### 2.4 Mean Zero-Crossing Wave Period ( $T_z$ )

The zero-crossing wave period refers to the time between the two wave points when the wave height is zero, and the wave is either going up (up-crossing) or down (down-crossing).

Likewise, the mean zero-crossing period is defined as:

$$\bar{T}_z = \frac{1}{N} \sum_{i=0}^N t_i \quad (6)$$

where  $t_i$  refers to the zero-crossing periods of all waves in the corresponding surface elevation slices (i.e., zero-crossings determined by linear interpolation).

### 2.5 Power Spectral Density (PSD)

In some spectra, the total 'signal energy' is defined as:

$$E_s = \int_{-\infty}^{+\infty} |y(t)|^2 dt \quad (7)$$

where  $y(t)$  refers to some quantity measured over time,  $t$ . For example, if  $y(t)$  is taken to be wave height, then the units of signal energy are  $m^2s$ . Note that the signal energy should be a bounded process, and thus,  $y(t)$  should be a product of a deterministic process, *i.e.*, non-random and with a clear start and finish criteria.

Assuming  $y(t)$  as an integrable function and Fourier transform of  $y(t)$ ,  $Y(f)$  exists, the transformation into the frequency domain is given by

$$Y(f) = \int_{-\infty}^{\infty} y(t) \exp^{-i2\pi ft} dt \quad (8)$$

Following this definition, the power spectral density or signal spectral density is defined as the square of the modulus of  $Y(f)$ , *i.e.*,

$$S_E(f) = |Y(f)|^2 \quad (9)$$

It results in a similar expression to Equation 7 but in the frequency domain.  $S_E(f)$  will provide signal energy density at frequency  $f$ , and if  $y(t)$  is wave height, then its unity will be  $m^2s^2$ . After calculating spectral density for each frequency, we take the total power spectral density in the wave spectra.

## 2.6 Other Wave Properties

Other wave properties studied were mean wave direction ( $\theta$ ), directional spreading ( $\sigma$ ), skewness, and kurtosis. To calculate various properties of the distribution, we use the method proposed by Kuik *et al.* [15]. The Kuik *et al.* estimate of the kurtosis and skewness used in this paper is based on the integration over the frequency bands from 0.025 Hz to 0.580 Hz over the bulk Fourier moments  $a_1, b_1, a_2, b_2$  weighted by the energy density. Note that Fourier moments refer to the coefficients of sines and cosines calculated from the waves after Fourier transform.

$$\begin{bmatrix} a_1 \\ b_1 \\ a_2 \\ b_2 \end{bmatrix} = \frac{1}{E^b} \int_{0.025}^{0.580} \left( df E_r(f) \begin{bmatrix} a_1(f) \\ b_1(f) \\ a_2(f) \\ b_2(f) \end{bmatrix} \right) \quad (10)$$

where  $E^b$  is the variance with

$$E^b = \int_{0.025}^{0.580} df E_r(f) \quad (11)$$

afterward, we calculate

$$\theta = \tan^{-1}\left(\frac{b_1}{a_1}\right) \quad (12)$$

$$m_1 = (a_1^2 + b_1^2)^{1/2} \quad (13)$$

$$\sigma = [2(1 - m_1)]^{1/2} \quad (14)$$

$$m_2 = a_2 \cos(2\theta) + b_2 \sin(2\theta) \quad (15)$$

$$n_2 = b_2 \cos(2\alpha) - a_2 \sin(2\alpha) \quad (16)$$

$$skewness = \gamma = \frac{-n_2}{[(1 - m_1)/2]^{3/2}} \quad (17)$$

$$kurtosis = \delta = \frac{6 - 8m_1 + 2m_2}{[2(1 - m_1)]^2} \quad (18)$$

In (10), the bulk Fourier moments are derived from calculating the skewness and kurtosis. We take the integration of the Fourier moments multiplied by energy [21] and bandwidth. It is then normalized by dividing it with variance calculated in (11). Afterward, we use (12) to (16) to find different parameters, which are used to calculate skewness and kurtosis. Subsequently, we calculate the skewness and kurtosis in (17) and (18), respectively. Note that (12) and (14) give wave direction and directional spread, respectively.

## 3. EXPERIMENTAL SETUP

### 3.1 Dataset

The dataset used in this study contains the buoy data obtained from the CDIP website [22]. The data is obtained in various formats like time-series, 30-min averaged, and spectral data.

We used 1,049,902 points for the training dataset and 449,958 points for the testing dataset, which accounts for 70% and 30% of the total data, respectively. The data was separated based on temporal ordering. Thus, the data in the testing dataset contains the data that is obtained after the time of the data in the benchmark dataset.

### 3.2 Features

The features used in this study consist of day of the month, time of day, month of the year, significant wave height ( $H_{m0}$ ), mean wave period ( $T_a$ ), dominant wave period ( $T_p$ ), wave direction ( $D_p$ ), Zero up-crossing period ( $T_z$ ), Directional Spread, Power Spectral Density (PSD), depth, skewness, and kurtosis.

Table 1: Statistical Properties of the dataset

Variable	Minimum	Mean	SD	Maximum
depth	11.0	287.75	522.28	1920.0
$H_{m0}$	0	1.02	0.55	39.04
$T_z$	1.08	5.57	1.74	28.57
$T_p$	0	10.35	4.11	40
$D_p$	-12.07	0.04	0.21	85.1
$T_a$	1.82	6.35	2.10	29.18
Spread	21.76	43.26	7.14	75.36
PSD	1.16e-5	1.80	5.33	4134
Skew	-770.12	-1.0e-8	1.22	587.43
Kurtosis	-966.88	1.51	4.12	502.49

### 3.3 Data filtering

Field measurement of waves is subject to various errors that must be removed to obtain a high quality and reliable dataset. Some examples of the errors include experimental error, buoys getting carried away with the waves, underestimating wave heights, biofouling, etc. Thus, a stringent QC procedure is required to obtain a good dataset in which various machine learning methods can be applied.

The CDIP buoys automatically give the data separated into 30-min intervals. The usage of 30-min intervals lies in how the waves measured are stationary and reasonable predictions can be made. The buoy automatically flags questionable, bad, or CDIP runs

missing data points in the same domain as the vertical displacement and other shore-side QC procedures. The 30-min sea with an error flag was removed. For the erroneous data that was not identified by the buoy or CDIP QC procedure, a series of filters were employed to screen and remove the outliers. The filtering procedure has been used widely throughout the literature.

- 1) Individual waves with zero-crossing wave period  $> 25$ .
- 2) Rate of change of surface elevation  $Sy$  exceeded by a factor of 2.

$$Sy = \frac{2\pi\sigma}{T_z} \sqrt{2\ln N_z}$$

where  $\sigma$  is the standard deviation of the surface elevation  $\eta$  and  $N_z$  is the number of zero up crossing periods ( $T_z$ ).

- 3) Absolute crest or trough elevation greater than 5 times the standard deviation of the 30-min water surface elevation.
- 4) A single zero-crossing containing  $> 2304$  points.
- 5) Wave crest elevation  $\eta_c > 1.5 H_s$ .
- 6) Horizontal buoy excursion  $\Delta x$ ,  $\Delta y$  where  $\Delta x > 1.8 H_s$  or  $\Delta y > 1.8 H_s$ .

### 3.4 Cross-validation

A common technique used for cross-validation while training machine learning methods is KFold cross-validation. In KFold cross-validation, the data is first shuffled, then divided into various segments, and machine learning methods after that are applied by keeping one part as a test dataset, the rest as training, and then repeating the procedure for all folds. The main disadvantage of using this method is that dependency among the observations is not taken into account, and thus, the validation procedure generates overly optimistic estimations or poor generalization ability of the predictive models. We use the hv-block cross-validation procedure [23], first proposed by Racine and used for stationary time series data. The procedure is like the KFold validation, except that there is no random shuffling of the observations. Thus, it renders K blocks of contiguous observations in their natural order. Afterward, while testing the models, adjacent observations between the training and test sets are removed to create a gap between the two sets and increase independence among the observations. The general procedure for hv-block cross-validation is illustrated in Figure 1.

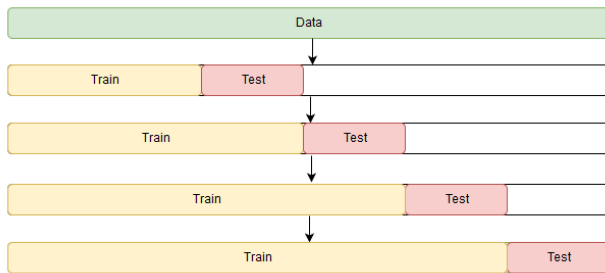


Figure 1: Setup for hv-blocked cross-validation

### 3.5 Removing Trend from the Data

To remove trends from the data, we used differencing. Differencing is defined as a method in which, instead of predicting the value, the predictor is trained to predict how much the next value will differ from the current one. This step

automatically performs standardization of data and removes any trend or seasonality from the data, thus making the predictors more robust and accurate. The procedure of differencing can be shown as

$$\begin{aligned}\bar{X}_1 &= X_k - X_0 \\ \bar{X}_2 &= X_{k+1} - X_1 \\ &\dots \\ \bar{X}_{n-k} &= X_n - X_k\end{aligned}$$

Where  $X_n$  refers to the original output values,  $\bar{X}_n$  refers to the differenced value for prediction, and  $k$  refers to the steps used for predictions. The total data size of  $n$  would thus produce  $n - k$  points for the training and test dataset.

Afterward, the term that was removed earlier is then added back to the results produced from the machine learning algorithms to produce the final predictions.

### 3.6 Evaluation Metrics

To measure the performance of our model and to compare the results with other methods, we employ various metrics like Root Mean Squared Error (RMSE), Mean Absolute Error (MAE), Variance, R2 Score, Scatter Index (SI), Correlation Coefficient (CC), Bias, and Hanna and Heinold (HH) Indicator. Note that RMSE, Bias and MAE are measured in *meters*, Variance in *meters*<sup>2</sup> and SI, R2 Score, CC, and HH are nondimensional.

Table 2: Evaluation Metrics and their calculations

Name	Mathematical Formula
RMSE	$RMSE = \sqrt{\frac{\sum_{i=1}^N (x_i - \hat{x}_i)^2}{N}}$
MAE	$MAE = \frac{1}{N} \sum_{i=1}^N  x_i - \hat{x}_i $
Variance	$Variance = \frac{\sum_{i=1}^N (x_i - x_m)^2}{N}$
R2 score	$R2 = 1 - \frac{\sum_{i=1}^N (x_i - \hat{x}_i)^2}{\sum_{i=1}^N (x_i - x_m)^2}$
SI	$SI = \frac{RMSE}{\frac{1}{n} \sum_{i=1}^N x_i}$
CC	$CC = \frac{\sum_{i=1}^N (x_i - x_m)(\hat{x}_i - \hat{x}_m)}{\sqrt{\sum_{i=1}^N (x_i - x_m)^2 \sum_{i=1}^N (\hat{x}_i - \hat{x}_m)^2}}$
Bias	$Bias = \frac{1}{N} \sum_{i=1}^N (x_i - \hat{x}_i)$
HH	$HH = \sqrt{\frac{\sum_{i=1}^N (x_i - \hat{x}_i)^2}{\sum_{i=1}^N x_i \hat{x}_i}}$

In the preceding table,  $x_i$  refers to the measured value,  $\hat{x}_i$  refers to the predicted value at position  $i$ ,  $x_m$  refers to the mean of actual values,  $\hat{x}_m$  refers to the mean of predicted values, and  $N$  refers to the number of elements, respectively.

## 4. RESULTS

The machine learning methods were tested for forecasting significant wave height for various forecast range. It is noted that 10-fold hv-blocked cross-validation was used for training, and then the optimum parameters were identified. After calculating the best parameters, we train the data on the training set and predict the data using the test set. Note that each window contains 30-min data, and thus, for day-1 forecasting, the algorithm forecasts 48 steps and so on.

### 4.1 Significant Wave Height

#### 4.1.1 Adjusted R2 score

We observe from Figure 2 that the Adjusted R2 score for significant wave height decreases in general as the forecast time increases. The highest decrease is from day-0 to day-1 forecasting, where it drops from 0.999 to 0.915 for LightGBM and 0.936 for Extra Trees. However, after that, even though there are some fluctuations, the R2 score does not change significantly. A similar trend is observed for both training and test dataset. Note that R2 scores close to 1 are considered to be good for predictions, and since on all the time ranges tested, the performance is greater than 0.9, the predictions made by the algorithms are close to the real measurements.

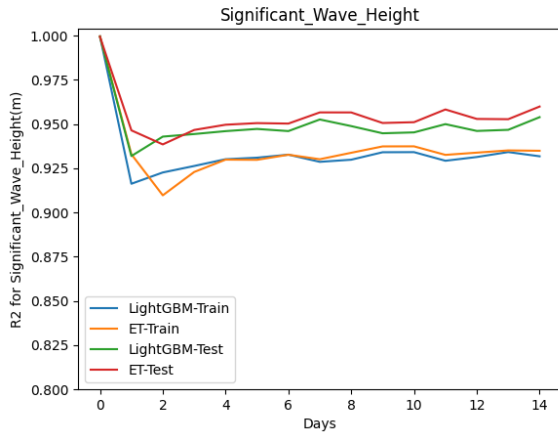


**Figure 2: Adjusted R2 score for the significant wave heights for various forecast range**

#### 4.1.2 Root Mean Squared Error (RMSE)

In Figure 3, the RMSE of the machine learning algorithms generally increases for both training and test datasets as the forecast time increases. The RMSE value increases the most from day-0 to day-1, where it increases from 0.01m to 0.16m for LightGBM and 0.14m for Extra Trees. After that, even though there are some fluctuations, the RMSE values do not change significantly. Note that for RMSE, values close to 0 are considered good. Thus, the performance of both algorithms can be considered excellent in terms of RMSE.

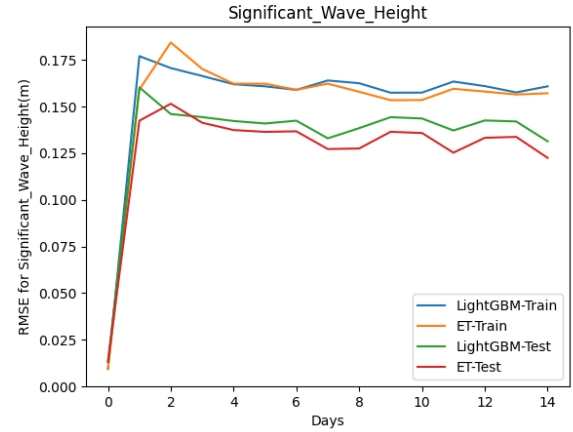


**Figure 3: Root mean squared error (RMSE) score for the significant wave heights for various forecast range**

#### 4.1.3 Variance

From Figure 4, we observe that in general, the variance for both classifiers decreases rapidly at first, from day-0 to day-1, and then shows limited change afterward. In the case of Extra Trees, the variance is 0.999 at day-0 and 0.933 at day-1 on the training dataset and 0.999 at day-0 and 0.947 at day-1 on the test dataset. Similarly, for the LightGBM, the variance is 0.999 at day 0 and 0.916 at day 1 for the training dataset and 0.999 at day 0 and 0.931 at day 1 for the test dataset. After that, the variance shows periodic fluctuations, although they are close to 0.950 for Extra Trees and 0.930 for LightGBM. It is worth noting that algorithms with a variance close to 1 are considered excellent for prediction.

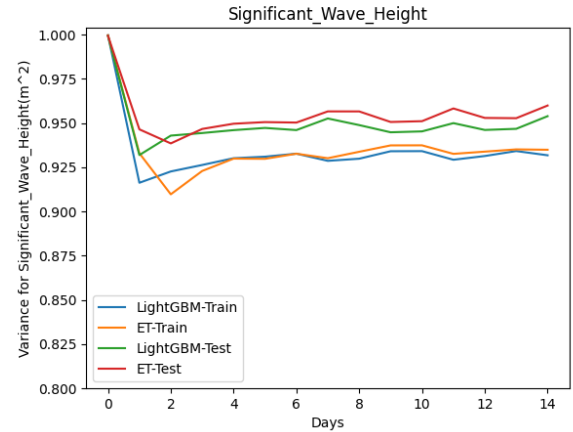


**Figure 4: Variance for the significant wave heights for various forecast range**

#### 4.1.4 Correlation Coefficient (CC)

In Figure 5, the CC for both algorithms decreases from day-0 to day-1 but shows periodic fluctuations afterward, even though the values are not changing significantly. In the case of Extra Trees, the CC remains close to 0.975 but remains close to 0.965 for the LightGBM algorithm. It should be noted that a CC value close to 1 is considered excellent.

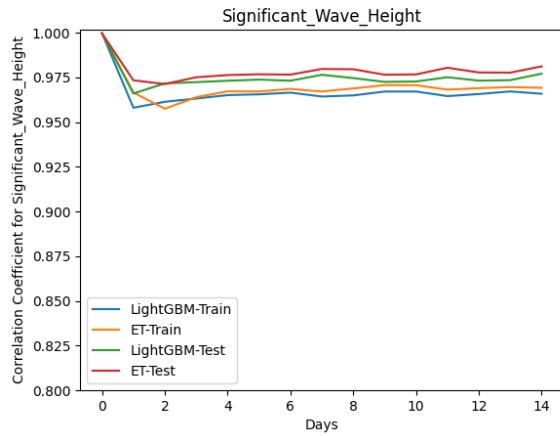


**Figure 5: Correlation Coefficient (CC) for significant wave heights for various forecast range**

#### 4.1.5 Scatter Index (SI)

Figure 6 shows that in general, the SI for both classifiers increases rapidly till about 5 days and then remains somewhat stagnant afterward even though the values fluctuate randomly. The SI values remain within 0.16 for LightGBM and 0.15 for Extra Trees for all the windows tested. Recall that for SI, values close to 0 are considered excellent.

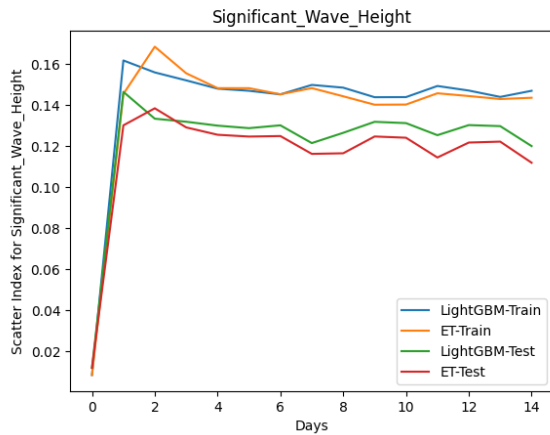


**Figure 6: Scatter Index (SI) for significant wave heights for various forecast range**

#### 4.1.6 Bias

In Figure 7, the bias for the models generally shows fluctuations but no periodic trend. However, we can observe that the Extra Trees algorithm's bias is higher than that of LightGBM even though both have bias values close to 0 for both training and test dataset. It is pointed out that Bias values close to 0 are considered excellent for prediction purposes.

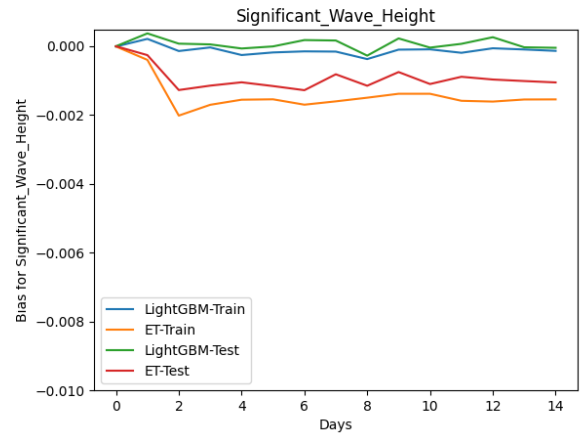


**Figure 7: Bias score for significant wave heights for various forecast range**

#### 4.1.7 Hanna and Heinold (HH) Indicator

Figure 8 shows that, in general, the HH values increase as the forecast time increases. However, the highest increase is seen from day-0 to day-1 when both algorithms go from HH values of nearly 0 to around 0.14. After that, although the values fluctuate randomly, they don't change significantly. Note that the HH values close to 0 are considered excellent for prediction purposes.

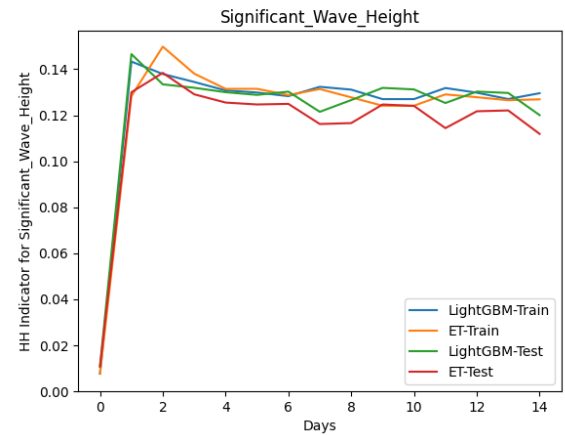


**Figure 8: Hanna and Heinold (HH) Indicator for significant wave heights for various forecast range**

#### 4.1.8 Mean Absolute Error (MAE)

Figure 9, shows that in general, the Mean Absolute Error (MAE) of the machine learning algorithms increases for both training and test datasets as the forecast window increases. However, after the first day, the MAE values remain consistent, around 0.10 for LightGBM and 0.08 for ET.

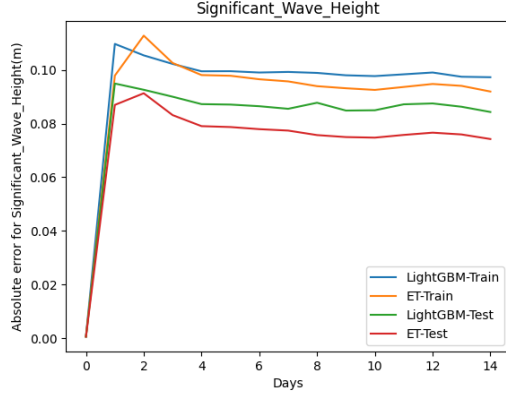


Figure 9: Mean Absolute Error (MAE) for the significant wave heights for various forecast range

## COMPARISON OF SIGNIFICANT WAVE HEIGHT PREDICTION WITH OTHER STATE-OF-THE-ART METHODS

In this section, we compare our method with other commonly used methods for 1 day ahead forecasting. Note that since Bidlot *et al.* [24] tested the other methods using buoy data from June to August 2007, we utilize data from January 2001 to June 2007 as a training dataset and June to August 2007 as the test dataset. The models compared are European Centre for Medium-range Weather Forecasts (ECMWF) [24-26], Met Office (MO) [27], Fleet Numerical Meteorology and Oceanography Centre (FNMOC), Meteorological Service of Canada (MSC) [28-30], National Centers for Environmental Prediction (NCEP) [10, 11, 31, 32], Meteo France (MF) [33-36], Deutscher Wetterdienst (DWD) [37], Bureau of Meteorology (BoM) [24, 38-40], Service Hydrographique et Oceanographique de la Marine (SHOM) [41], Japan Meteorological Agency (JMA) [42], Korea Meteorological Administration (KMA) [43]. Note that all the methods compared are global models. Moreover, the other models take the data from (0-12 hours) to predict up to 24 hours ahead, which is only one step forward prediction.

In contrast, we perform 48 steps ahead prediction while only taking the wave information from (0-0.5 hours). Even though we take the individual prediction window of 30 minutes, which is less stationary than the 12-hour window, our method performs significantly better. It is important to note that we only compare our approach to numerical methods since earlier machine learning methods were shown to underperform numerical approaches. The results obtained can be summarized in Table 3.

Table 3: Comparison of the proposed method with other state-of-the-art methods

Method	SI	Bias(m)	CC	RMSE(m)
ECMWF	0.151	-0.02	0.95	0.25
MetO	0.210	0.20	0.92	0.40
FNMOC	0.192	0.04	0.94	0.32
NCEP	0.186	0.11	0.94	0.33
MF	0.231	0.22	0.89	0.44
DWD	0.202	0.04	0.92	0.34
BoM	0.226	0.03	0.89	0.38

SHOM	0.180	0.00	0.93	0.30
JMA	0.209	-0.18	0.91	0.40
KMA	0.305	0.05	0.79	0.50
Our Method	<b>0.130</b>	<b>-0.002</b>	<b>0.97</b>	<b>0.14</b>

In the preceding table, the best values are highlighted in bold. Note that our proposed method has a very low Scatter Index (SI), bias, and RMSE value. Likewise, the Correlation Coefficient (CC) of the proposed method is very high compared to the other methods, suggesting that the proposed method can be used to forecast the significant wave height in oceans.

## 5. DISCUSSION

The results section shows that in general, for both Extra Trees and LightGBM, the performance of the algorithms decreases sharply from day 0 to day 1 but remains consistent afterward with small fluctuations. The small fluctuations can be attributed to the feature of the dataset and, to some extent, to the noise inherent in the dataset. Note that although the QC procedure adopted in the paper captures many errors, there will be some other errors that are still not caught and might be captured when studying other higher-order moments like skewness and kurtosis, which are not investigated in this paper.

The Extra Trees, which performs bagging on the data, performs better than LightGBM, which performs boosting on the data. The comparatively better performance of ET shows that the data contains more variance error than bias, which is often due to noise in the dataset.

Next, we plot the feature importance, computed by the Extra Trees algorithm for significant wave heights. The results obtained are shown in Figure 10.

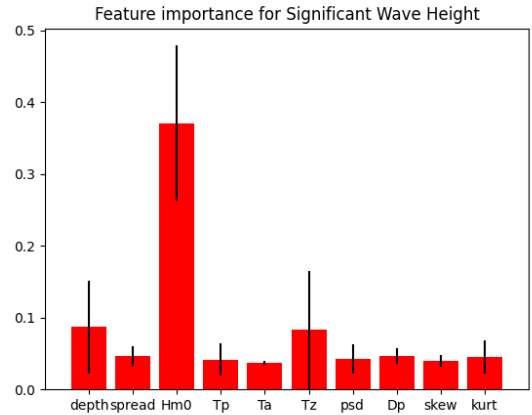


Figure 10: Feature importance of various features for 1 day ahead forecasting of significant wave heights

In Figure 10, significant wave height has the highest feature importance of 0.370. Depth has the second-highest feature importance of 0.087. Directional spread, zero-crossing period, dominant wave period, power spectral density, mean wave period, wave direction, skewness, and kurtosis have feature importance of 0.046, 0.042, 0.036, 0.083, 0.042, 0.047, 0.040, and, 0.045 respectively.

The two machine learning methods chosen in this paper are LightGBM, and ET, minimize bias and variance, respectively.



LightGBM performs boosting on the data, and ET performs bagging. The superior prediction capability of ET algorithm suggests that the data is noisy.

Our proposed algorithm has a better predictive capability for forecasting wave height than other state-of-the-art methods, both statistical and numerical. Despite using only, the variables available from the spectra of the buoys, our method performs better than other methods that take wind speed and air/water temperature, and other variables into account. Our algorithm's superior performance can be attributed to cross-validation, data filtering, and differencing.

First, we use various data filtering methods to get the most accurate data for training and test purposes. These methods are widely used in physical oceanography to filter outliers in the buoy wave data. We use hv-blocked cross-validation to ensure that the data's temporal order is not disturbed while training the model. After that, we compare various machine learning algorithms on the features generated and found that ET, a tree-based machine learning algorithm, works better for forecasting using various wave features derived from the buoys.

Note that for 1 day ahead of forecasting, while only taking the data from 30-min interval, the machine learning methods tested (ET and LightGBM) can forecast up to 14 days (which is the setup of our experiment) without an abrupt decrease in prediction performance. When the time period is taken is longer, the data is usually stationary, and it is easier to make predictions. Unlike the numerical methods compared in this paper, which use 12-hour intervals, our proposed algorithm can forecast the significant wave heights in 30-min intervals and still have comparable performance. Moreover, the performance of both algorithms is similar to the state-of-the-art methods for 48 steps ahead prediction, whereas the global methods mentioned in Section 6 only perform one step ahead predictions. The robust performance of the machine learning methods, comparable to the state-of-the-art numerical methods, suggests that machine learning methods, combined with spectral features and blocked cross-validation procedure, can be used to forecast various wave properties.

## 6. CONCLUSION

In theory, wave forecasting can be done using model equations of empirical relationships between various wave parameters. Compared to the nonlinear differential equations, machine learning methods provide similar models with lower computational complexity and computation time.

This study analyzed various methods for quality control of data and cross-validation for time data. The methods, combined with the machine learning algorithms, allowed us to forecast significant wave heights for various time ranges without an abrupt decrease in prediction performance over time. Likewise, the use of tree-based algorithms explored in this paper (LightGBM and ET) give feature importance, which helps quantify the impact of the features and help understand how the algorithm is making decisions. Moreover, the data collected from CDIP buoys are very accurate after the application of the QC procedure, thus allowing for improved performance. The QC methods, block cross-validation, and machine learning methods help us predict significant wave heights, a nonlinear phenomenon with performance comparable to the state-of-the-art methods. Future studies will incorporate ocean currents, wind, and other wave parameters for wave and wind forecasting.

We posit that similar algorithms and setup would allow for forecasting wave heights and other wave properties on various

other nonlinear media allowing for early forecasting of such waves.

## 7. ACKNOWLEDGMENTS

This work was supported in part by the U.S. Navy (Office of Naval Research) under contract N00173-16-2-C902.

## 8. REFERENCES

- [1] H. v. Haren, "Grand Challenges in Physical Oceanography," *Frontiers in Marine Science*, vol. 5, no. 404, October 29 2018, 2018.
- [2] W. M. Harald Ulrik Sverdup, "Wind, sea and swell. The Theory of relations for forecasting," *U.S. Navy Hydrographic Office*, vol. Publication No. 601, March 1947, 1947.
- [3] P. F. J. L. Nadia Pinardi, Kenneth H. Brink, Ruth H. Preller, "The Sea: The Science of Ocean Prediction," *Journal of Marine Research*, vol. 75, no. 3, pp. 101-102, April 2007, 2017.
- [4] A. S. Omer San, "An Efficient Coarse Grid Projection Method for Quasigeostrophic Models of Large-Scale Ocean Circulation," *International Journal of Multiscale Computational Engineering*, vol. 11, no. 5, August 2013, 2013.
- [5] A. C. Hendrik L. Tolman, "Automated grid generation for WAVEWATCH III," *NOAA/NWS/NCEP/MMAB Technical Note*, vol. 254, April 2007, 2007.
- [6] J. M. W. Erick Rogers, Kaihatu, Larry Hsu, R.E. Jensen, James Dykes, K. Todd Holland, "Forecasting and hindcasting waves with the SWAN model in the Southern California Bight," *Coastal Engineering*, vol. 51, no. 1, September 2006, 2006.
- [7] H. L. Tolman, "The numerical model WAVEWATCH: a third generation model for the hindcasting of wind waves on tides in shelf seas," *Communications on Hydraulic and Geotechnical Engineering, Delft University of Technology*, vol. 89, no. 2, April 1989, 1989.
- [8] H. L. Tolman, "User manual and system documentation of WAVEWATCH III R version 4.18," *NOAA/NWS/NCEP/EMC Technical Note*, vol. 316, February 2014, 2014.
- [9] H. L. Tolman, "A Third-Generation Model for Wind Waves on Slowly Varying, Unsteady, and Inhomogeneous Depths and Currents," *Journal of Physical Oceanography*, vol. 21, no. 6, June 1 1991, 1991.
- [10] H. L. Tolman, "Treatment of unresolved islands and ice in wind wave models," *Ocean Modelling*, vol. 5, no. 3, 2003, 2003.
- [11] J.-H. G. M. A. Yung Y. Chao, Hendrik L. Tolman, "An Operational System for Predicting Hurricane-Generated Wind Waves in the North Atlantic Ocean," *Weather and Forecasting*, vol. 20, no. 4, pp. 652-671, August 01 2005, 2005.
- [12] G. S. Silvana Ilie, Robert M. Corless, "Adaptability and computational complexity in the numerical solution of ODEs," *Journal of Complexity*, vol. 24, no. 3, June 2008, 2008.
- [13] A. J. M.C. Deo, A.S. Chaphekar, R. Ravikant, "Neural networks for wave forecasting," *Ocean Engineering*, vol. 28, no. 7, pp. 889-898, July 2001, 2001.
- [14] A. E. A. M. J. Mahjoobi, "Prediction of significant wave height using regressive support vector machines," *Ocean Engineering*, vol. 36, no. 5, pp. 339-347, April 2009, 2009.



- [15] A. E.-S. J. Mahjoobi, "An alternative approach for the prediction of significant wave heights based on classification and regression trees," *Applied Ocean Research*, vol. 30, no. 3, July 2008, 2008.
- [16] A. S. A. Illa Rizianiza, "Prediction of significant wave height in The Java Sea using Artificial Neural Network," *International Seminar on Intelligent Technology and Its Applications (ISITIA)*, April 2015, 2015.
- [17] A. H. A. Moussa Sobh Elbisy, Abdulkarim Hatim Natto, Abdullah Abdulaziz Baksh, Ahmad Fetais Almaliki, Mohammad Awwad Alharthi, Abdelrahman Osama Hassan, "Prediction of Daily Tidal Levels along the central coast of Eastern Red Sea using Artificial Neural Networks," *International Journal of GEOMATE*, vol. 19, no. 76, pp. 54-61, December 2020, 2020.
- [18] M. S. Elbisy, "Sea Wave Parameters Prediction by Support Vector Machine Using a Genetic Algorithm," *Journal of Coastal Research*, vol. 31, no. 4, July 2015, 2015.
- [19] Y. H. W.Y. Duan, L.M. Huang, B.B. Zhao, M.H. Wang, "A hybrid EMD-SVR model for the short-term prediction of significant wave height," *Ocean Engineering*, vol. 124, no. 15, September 15 2016, 2016.
- [20] G. A. Somayeh Mafi, "Forecasting hurricane wave height in the Gulf of Mexico using soft computing methods," *Ocean Engineering*, vol. 146, no. 1, December 2017, 2017.
- [21] M. S. Longuet-Higgins, "The Directional Spectrum of Ocean Waves, and Processes of Wave Generation," *Proceedings of the Royal Society of London. Series A, Mathematical and Physical Sciences*, vol. 265, January 30 1962, 1962.
- [22] R. A. H. Hilary F. Stockdon, Peter A. Howd, Asbury H. Sallenger Jr., "Empirical parameterization of setup, swash and runup," *Coastal Engineering*, vol. 53, no. 7, pp. 573-588, May 2006, 2006.
- [23] J. Racine, "Consistent cross-validated model-selection for dependent data: hv-block cross-validation," *Journal of Econometrics*, vol. 99, no. 1, pp. 39-61, November 2000, 2000.
- [24] J.-G. L. Jean Bidlot *et al.*, "Inter-Comparison of operational wave forecasting systems," *10th International Workshop of Wave Hindcasting and Forecasting, Hawaii*, December 2006, 2006.
- [25] P. A. E. M. J. J.R. Bidlot, S. Abdalla, "A revised formulation of ocean wave dissipation and its model impact," *ECMWF Technical Memoranda*, vol. 509, January 2007, 2007.
- [26] P. A. E. M. Janssen, "Progress in ocean wave forecasting," *ECMWF Technical Memoranda*, vol. 529, June 2007, 2007.
- [27] B. Golding, "A wave prediction system for real-time sea state forecasting," *Quarterly Journal of the Royal Meteorological Society*, April 1983, 1983.
- [28] R. Lalbeharry, "Evaluation of the CMC regional wave forecasting system against buoy data," *Atmosphere-Ocean*, vol. 40, no. 1, July 21 2010, 2010.
- [29] S. D. R. Lalbeharry, H. Ritchie, A. Macafee, L. Wilson, "Wave simulation of hurricanes using blended winds from a parametric hurricane wind model and CMC weather prediction model," *Proceedings of 5th International Symposium on Ocean Wave Measurement and Analysis*, July 3-7 2005, 2005.
- [30] J. M. S. Desjardins, R. Lalbeharry, "Examination of the impact of a coupled atmosphere and ocean wave system. Part I: Atmospheric aspects," *Journal of Physical Oceanography*, vol. 30, no. 2, pp. 402-415, February 01 2000, 2000.
- [31] H. L. T. e. al., "Development and Implementation of Wind-Generated Ocean Surface Wave Models at NCEP," *Weather and Forecasting*, vol. 17, no. 2, pp. 311-333, April 01 2002, 2002.
- [32] H. L. Tolman, "Alleviating the Garden Sprinkler Effect in wind wave models," *Ocean Modelling*, vol. 4, no. 3-4, pp. 269-289, June 2002, 2002.
- [33] D. H. Beatrice Frandon, Jean-Michel Lefevre, "Comparision Study of a Second-Generation and of a Third-Generation Wave Prediction Model in the Context of the SEMAPHORE Experiment," *Journal of Atmospheric and Oceanic Technology*, vol. 17, no. 2, pp. 197-214, February 01 2000, 2000.
- [34] J.-M. L. Chaifih Skandrani, Pierre Queffeuilou, "Impact of multi-satellite Altimeter Data Assimilation on Wave Analysis and Forecast," *Marine Geodesy*, vol. 27, no. 3-4, pp. 511-533, June 01 2004, 2004.
- [35] H. B. Daniele Hauser *et al.*, "The FETCH experiment: An overview," *Journal of Geophysical Research*, February 13 2003, 2003.
- [36] P. D. C. J.-M. Lefevre, "Chapter 7 Ocean Surface Waves," *International Geophysics*, vol. 69, pp. 305-328, 2001, 2001.
- [37] D. S. Arno Behrens, "The wave forecast system of the "Deutscher Wetterdienst" and the "Bundesamt fur Seeschifffahrt und hydrographie": A verification using ERS-1 altimeter and scatterometer data," *Ocean Dynamics*, vol. 46, no. 2, pp. 131-149, May 1994, 1994.
- [38] E. W. S. Diana J.M. Greenslade, Jeff D. Kepert, Graham R. Warren, "The impact of the assimilation of scatterometer winds on surface wind and wave forecasts," *Journal of Atmospheric and Oceanic Science*, vol. 10, no. 3, pp. 261-287, January 26 2007, 2007.
- [39] J. D. K. Eric W. Schulz, Diana J.M. Greenslade, "An Assessment of Marine Surface Winds from the Australian Bureau of Meteorology Numerical Weather Prediction Systems," *Weather and Forecasting*, vol. 22, no. 3, pp. 613-636, June 01 2007, 2007.
- [40] L. C. Bender, "Modification of the Physics and Numerics in a Third-Generation Ocean Wave Model," *Journal of Atmospheric and Oceanic Technology*, vol. 13, no. 3, pp. 726-750, June 01 1996, 1996.
- [41] T. H. C. H. Fabrice Ardhuin, Kristen P. Watts, Gerbrant Ph van Vledder, R. Jensen, Hans C. Graber, "Swell and Slanting-Fetch Effects on Wind Wave Growth," *Journal of Physical Oceanography*, vol. 37, no. 4, pp. 908-931, April 01 2007, 2007.
- [42] N. K. K. Ueno, "The development of the third generation wave model MRI-III," *Proceedings of 8th International Workshop on Wave Hindcasting and Forecasting*, 2004, 2004.
- [43] D.-U. L. Sangwook Park, Jang-Won Seo, "Operational Wind Wave Prediction System at KMA," *Proceedings on JCOMM Scientific and Technical Symposium on Storm Surges*, October 2-6 2007, 2008.

## Reproducibility

The data was accessed on 9/18/2020 on 16:30 from <https://cdip.uscd.edu> and the stations used are: 149, 150, 151, 152, 155, 158, 161, 165, 169, 172, 175, 181, 186, 189, 190, 191, 201, 203, 207, 208, 209, 210, 211, 212, 213, 214, 215, 216 and 217. The code can be downloaded from <https://github.com/ppokhrell/waves>. The parameters for the machine learning methods used are given in Table 4.

**Table 4: Parameters of LightGBM and Extra Trees for various windows**

Window	LightGBM			ET		
	n_estimators	min_samples_child	num_leaves	n_estimators	min_samples_leaf	min_samples_split
0	600	5	5000	1000	2	2
1	500	2	5000	950	2	2
2	650	2	5000	1100	2	2
3	600	5	5500	1000	2	2
4	700	2	5000	1000	2	2
5	800	5	6500	1000	2	2
6	700	5	5000	950	2	2
7	700	5	5000	1000	2	2
8	700	2	5000	1000	2	2
9	600	5	5500	1100	2	2
10	700	2	4500	1000	2	2
11	750	2	5000	1100	2	2
12	600	5	5000	1100	2	2
13	650	2	6500	1000	2	2
14	700	5	5000	1000	2	2

The preceding table shows various parameters for the machine learning methods used in this study. Note that for LightGBM, the search space for n\_estimators is [100, 1000], min\_samples leaf is [2, 500], and, num\_leaves is [100, 7000]. Similarly, in case of ET, the search space for n\_estimators is [100, 1200], min\_samples\_split is [2, 500], and, min\_samples\_leaf is [2, 500].